Robust Fractional PI Controller Design for Stand-Alone Microgrid under Load Variation: An Optimization-Based Approach

Asma DKHIL[*‡], Jihed HMAD[**], Messaoud AMAIRI[*], Manel CHETOUI[*], Hafedh TRABELSI[**]

[*] National Engineering School of Gabes (ENIG), Research Laboratory Modeling, Analysis and Control of Systems (LR16ES22), University of Gabes, Tunisia

[**] National Engineering School of Sfax (ENIS), CES Laboratory, University of Sfax, Tunisia

(asma1993.dekhil@gmail.com, Jihed.hmad@enis.tn, chetoui.manel@gmail.com, amairi.messaoud@ieee.org, hafedh.trabelsi@enis.tn)

‡ Corresponding Author; Asma Dkhil, National Engineering School of Gabes Tel: +216 22382549

asma1993.dekhil@gmail.com

Received: 07.08.2023 Accepted:15.09.2023

Abstract- The primary goal of power control in an autonomous Microgrid (MG) is to reduce power fluctuations caused by undesirable operational conditions. This paper presents a reliable control method for standalone-based Microgrids with a single power source, specifically focusing on output voltage control. The proposed approach is based on a robust Fractional-Order Proportional Integral (FO-PI) controller. To achieve accurate control of current and voltage, a comprehensive Voltage Source Converter (VSC) model is developed, and the controller is meticulously tuned. The fractional voltage controller ensures a specified phase margin and enhances system robustness. Controller parameters are obtained using the constrained optimization algorithm. The robustness of the proposed controller is assessed under various conditions including voltage reference changes, high resistive load variations, filter parameter adjustments, and nonlinear load perturbations. Simulation results are conducted using MATLAB/Simulink and they highlight the advantages of the FO-PI controller over the conventional PI controller, including reduced peak overshoot, improved response time, enhanced output voltage quality, and reduced total harmonic distortion. Furthermore, the fractional characteristics of the FO-PI controller enhance the robustness of the Voltage Source Converter system compared to the PI controller.

Keywords Standalone micro-grid, PI Controller, Fractional order PI Controller, constrained optimization, Uncertainties, Load variation.

1. Introduction

Traditional power generation sources, such as coal, oil, and natural gas, are centralized and often require the transmission of electric energy over long distances. However, distributed energy resources (DER) systems are recently gaining more and more importance in the world's energy supply. These DER systems are decentralized and can be located close to consumers. Various types of DER options exist, encompassing both renewable and non-renewable sources. These encompass wind turbines, thermal solar systems, solar photovoltaic (PV) installations, hydroelectric power, diesel generators, fuel cells, geothermal setups, and micro-turbines. Despite potential drawbacks like voltage control and protection system issues [45], adopting Distributed Generation (DG) offers numerous benefits, including minimized power losses, substantial reduction in the consumption of fossil fuels, education of emissions of greenhouse gases, prolonged postponement of investments required for expanding the transmission system and

enhanced Power Quality (PQ) achieved using inverter-based DG. Despite the benefits associated with DER, improper placement, and dimensioning of these units within distribution systems can lead to significant technical hurdles [46].

These technical challenges can have adverse effects on voltage management, the reliability of power supply, system stability, asset control, protection systems, and the occurrence of unwanted islanding events [45,46]. Additionally, DG can impact economic considerations. For instance, distribution companies partially offset their expenses by charging fees for grid connectivity. The introduction of DG units into the system could jeopardize this source of income.

Another notable key point deserving more detailed consideration pertains to heightened uncertainty when Distributed Energy Resources (DER) are in the mix, necessitating the integration of a capable and streamlined energy management system. In this context, it's essential to factor in the variability of DER power output, especially when they serve as backup units, as this variability may change over time. DER units are commonly situated either in areas with substantial load demand or at the terminus of feeders within radial distribution systems.

Distributed generation projects, influenced by factors like system topology and power output variability, impact system characteristics. Strategic placement of DG units in radial distribution systems improves voltage profiles, reduces overloads, cuts peak demand, and lowers greenhouse gas emissions. DG units transform passive networks into active microgrids, offering benefits such as delayed capacity expansions, increased reliability, and smoother load demand curves. [46,47]

The application of MGs aligns well with the objectives of an energy transition approach and allows efficient energy management [2,3]. MGs offer customers the opportunity to reduce greenhouse gas emissions and improve energy supply. They enable the deployment of a greater number of zero-emission electricity sources, thus promoting environmentally friendly energy production. The installation of autonomous off-grid MGs, known as standalone MGs, constitutes an alternative to extending the electricity grid to supply isolated areas where access to an electricity grid is not available, such as islands and isolated cities [4].

DER systems in microgrids are connected to the load through power electronic converters, such as voltage source converters. Fluctuations in load dynamics can lead to significant variations and unwanted harmonics within the system. These fluctuations negatively impact the power quality, pose risks to system functionality, and can cause noticeable distortions in voltage and current waveforms [5]. Therefore, maintaining high voltage quality, especially for critical loads under worst-case load variations, requires effective control of the VSC output voltage. The VSC's control architecture consists of an inner current regulator to manage the system's dynamics and an outer voltage regulator responsible for monitoring the AC reference voltage.

In linear circuits with only single-frequency sinusoidal currents and voltages, the power factor is defined by the phase shift of the current and voltage. However, nonlinear loads introduce harmonic currents in addition to the fundamental frequency AC [6,7], and the current waveform deviates from a pure sine wave and takes on a different shape.

In MG power systems, non-linear loads can include rectifiers, certain types of electric lighting, electronic devices like computers, printers, TVs, servers, and telecom devices that use switched-mode power supply (SMPS) technology, as well as welding equipment and variable speed drives. Furthermore, in addition to non-linear loads, MGs can suffer from significant levels of unbalanced conditions caused by the intermittency of energy sources.

However, the MG must perform efficiently even when subjected to nonlinear and unbalanced loads without experiencing any decline in performance [8]. According to the guidelines outlined in the IEEE standards [9,10], it is crucial to maintain the total harmonic distortion (THD) and the power factor within the standard values as presented in Table 1.

Table 1. IEEE and IEC standards.

Issue	IEEE 1547	IEC 61727
Frequency range	59.9Hz-60.5Hz	50 ± 1Hz
Power factor	0.90	0.90
Voltage range	88% - 110%	85% - 110%
Nominal power	30KW	10KW
Nominal voltage	(97V-121V)	(196V-121V)
Maximum current THD	5%	5%
Current injection	< 1 % Iout	< 1 % Iout

Several approaches have been developed to control distributed generation systems specifically designed for MG applications [11,12]. These approaches involve the utilization of various controllers to mitigate voltage fluctuations and harmonics, such as adaptive control [13], sliding mode control [14], neural network-based control [15,16], predictive control [17], and nonlinear control [18]. Additionally, many techniques have also been proposed to reduce the THD voltage of an inverter when facing nonlinear load conditions, including passive filters and active damping [19, 20].

However, it is important to note that these techniques are primarily designed for single-bus MGs, and their utility in multi-bus microgrid applications has not been extensively studied. In [21], various current and power-sharing management schemes for inverters are explored to mitigate the effects of unbalanced and nonlinear loads.

On the other hand, among the compensation strategies proposed in the existing literature, the repetitive control technique [22] is convenient for harmonic compensation. Traditionally, VSC applications have relied on various Proportional-Integral-Derivative (PID) controllers [23] and Proportional-Integral (PI) controllers as described in [24] [25]. However, these controllers are highly sensitive to

parameter fluctuations and may struggle to ensure satisfactory performance and robustness, particularly when faced with variations in system parameters and operational conditions [25,26].

To enhance the PI controller's performance over a wide operating range [27], the application of FO-PI controllers has been suggested. This approach offers resilience against system uncertainties and helps to reduce voltage THD while providing robust disturbance rejection. Fractional calculus-based controllers have become more interesting in both research and industrial applications due to their ability to improve closed-loop system performance under uncertain conditions [28]. Particularly for complex nonlinear systems, the fractional order integrator component of the PI controller adds a substantial amount of flexibility to the controller design [29]. It has recently been used in several electric power system applications, such as load frequency management, voltage control, and stability analysis [30].

In [31], the study focuses on investigating a decentralized control technique known as FO-PI control to stabilize the output voltage levels within a microgrid system. Additionally, [32] presents a control scheme that utilizes an optimal fractional proportional-integral controller to enhance power sharing for parallel inverters. The researchers demonstrate that the fractional controller exhibits local stabilization capabilities, effective power distribution among resources, and minimization of circulating current, all without relying on communication links between distributed generators (DGs). To tackle uncertainties within the system, a similar fractional order controller is proposed for a standalone three-phase voltage source converter in [33]. The suggested FO-PI controller was compared to the traditional PID controller and shown to be efficient in terms of resilience against uncertainties and high-frequency disturbances.

In [34], a novel approach for controller tuning in the LFC of microgrid systems with communication delays is proposed. The FOPI method has significantly better system robustness concerning model gain variations. Furthermore, the study [35] introduces a decentralized coordinated control strategy to regulate the output voltage of various distributed generation systems, including solid oxide fuel cell (SOFC), photovoltaic (PV) systems, and battery energy storage systems (BESS). This strategy incorporates two types of controllers: a modified fractional-order proportional-integral (MFO-PI) controller and a two-degree-of-freedom proportional-integral (2DOF-PI) controller.

On the other hand, to improve the efficient operation of DG systems and energy storage devices, [36] introduces an effective frequency controller based on fractional order proportional-integral-derivative (FO-PID) control. The MOEO (multi-objective external optimization) algorithm has been employed in this controller's design to reduce the frequency deviation and controller output signal. Recently, suggested single-objective evolutionary algorithms, such as Kriging-based surrogate modeling and real-coded population extreme optimization-based FO-PID controllers, as well as other techniques such as FO-PID/PID controllers based on non-dominated sorting genetic algorithm, have been defeated by the decentralized coordinated control strategy that includes the FO-PID-based frequency controller. In the same context, [37] proposes a Hybrid Fuzzy Fractional Order Cascade Integrated Proportional Filter (HFI-FOCPD), as an effective controller. To ensure active power balancing in integrated hybrid systems including solar panels, wind turbines, energy storage, and loads, this controller is precisely developed in the voltage-controlled loop of the DC bus.

This paper presents a robust FO-PI controller designed for three-phase standalone MGs with a single power source. The proposed controller includes detailed modeling of VSC to integrate inner current and voltage control. A constrained optimization approach is implemented for controller parameter adjustments. Several simulations are performed using MATLAB/SIMULINK to test the operation of the suggested FO-PI controller by considering various uncertainty and load variation scenarios. An in-depth analysis of the obtained results of the FO-PI controller in comparison with those of a typical PI controller is conducted to evaluate the performance and effectiveness of the proposed method.

The paper is structured as follows: Section II provides a comprehensive system description, including the modeling of the VSC connected to a load via an LC filter. Section III focuses on the development of methods for tuning the controller parameters. Section IV presents the simulation results of a standalone MG to demonstrate the effectiveness of the proposed controller in handling load variation and system parameter uncertainties.

1. System Description and Modeling

Figure 1 illustrates a schematic model of a voltage source converter connected to a load through an LC filter. The model contains a *DC* source with a V_{DC} input *DC* voltage, *L* is the inductor filter, *C* is the capacitor filter, and *R* corresponds to the equivalent resistance, which involves the filter inductor Ohmic losses and the VSC switch resistance. The output inverter current, denoted as $i_{inv} = i$, represents the current generated by the inverter. On the other hand, i_L refers to the VSC output current that flows after the capacitor.

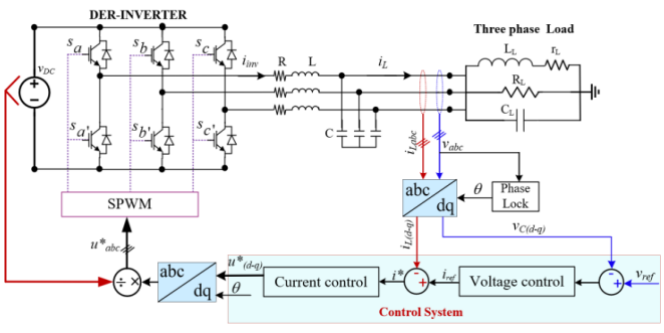

Figure 1. Schematic of the studied system.

The states of the semiconductor switches, which are IGBTs, alternate in a complementary manner. The control of these switching states is achieved through a PWM signal that incorporates binary values of 0 and 1.

The transformation from the *abc* frame to the Synchronous Reference Frame (SRF) *dq* allows the derivation of each three-phase variable. This transformation is expressed in the following equation:

$$\begin{pmatrix} i_d \\ i_q \end{pmatrix} = \begin{pmatrix} cos\theta & cos(\theta - \frac{2}{3}\pi) & cos(\theta + \frac{2}{3}\pi) \\ -sin\theta & -sin(\theta + \frac{2}{3}\pi) & -sin(\theta + \frac{2}{3}\pi) \end{pmatrix} \begin{pmatrix} i_a \\ i_b \\ i_c \end{pmatrix} \quad (1)$$

To ensure that the generated power matches the reference signal in terms of frequency and phase, a PLL can be employed. This monitoring and adjustment process is crucial as any deviations in frequency or phase can lead to instabilities and impact the overall system performance. Various phase loop control methods, such as Synchronous Reference Frame PLL (SRF-PLL), Enhanced PLL (EPLL), and Second Order Generalized Integrator PLL (SOGI-PLL), have been used in the literature [38]. For DG inverter applications, the SRF-PLL scheme presented in Figure 2 is widely used due to its simple implementation and effective design [39]. In situations where instability and perturbations are encountered, the SRF-PLL demonstrates superior performance compared to other techniques.

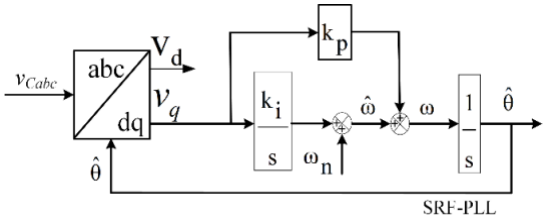

Figure 2. PLL synchronization.

Using the transformation, the output current and voltage of the inverter can be expressed as follows:

$$\begin{cases} \dot{i}_d = -\frac{R}{L} i_d + \omega i_q + \frac{1}{L}(v_d - v_{Cd}) \\ \dot{i}_q = -\frac{R}{L} i_q - \omega i_d + \frac{1}{L}(v_q - v_{Cq}) \\ \dot{v}_{Cd} = \omega v_{Cq} + \frac{1}{C}(i_d - i_{Ld}) \\ \dot{v}_{Cq} = -\omega v_{Cd} + \frac{1}{C}(i_q - i_{Lq}) \end{cases} \quad (2)$$

With: v_{dq}, i_{dq} are *d-q* axes of the inverter voltage and current output.

v_{cdq}, i_{Ldq}, are d-*q* axes filter voltage and current output; and ω is the inverter output angular speed.

3. Controller Tuning

Figure 3 presents a dual-control structure composed of an inner-loop current controller and an outer-loop voltage controller.

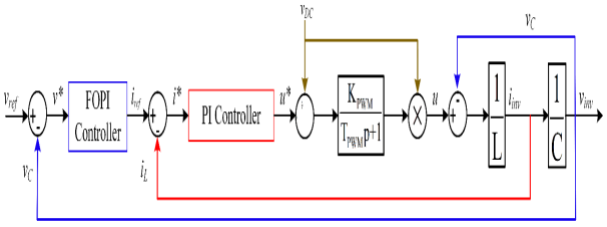

Figure 3. Control schematic of the studied system.

As shown in Figure 4 presenting the voltage and current control loop schematic, the outer voltage control is ensured by the controllers $G_v(s)$ considering the feedforward decoupling voltage $C\omega v_{cdq}$ and the current compensation iL_{dq}. Conversely, the controllers $G_c(s)$ ensure the inner current control by considering the feedforward decoupling ωL_{iLdq} current and the voltage compensation v_{cdq}.

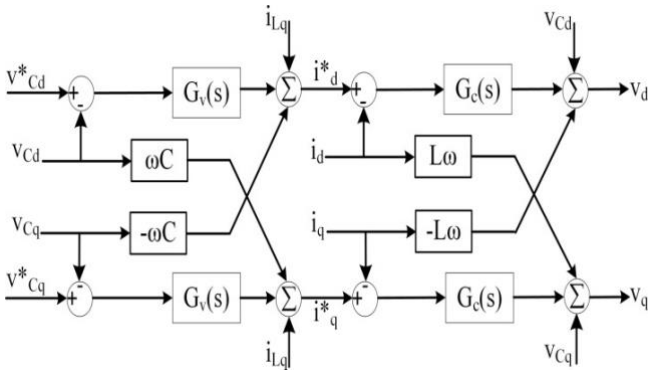

Figure 4. Schematic of voltage and current control loop**.**

3.1. *Inner Current Control*

In equation (2), there is cross-coupling between i_d and i_q, which needs to be decoupled to independently control the *d-q axis*. This decoupling is accomplished by introducing system input feedforward compensation.

$$\begin{cases} u_d = L\omega i_q + v_{Cd} \\ u_q = L\omega i_d + v_{Cq} \end{cases} \quad (3)$$

Where u_d and u_q are the d-q axis controller output.

The transfer function of the system is presented as follows:

$$H(s) = \frac{1}{Ls + R} \quad (4)$$

and the current controller is:

$$G_c(s) = K_{pc} + \frac{K_{ic}}{s} \qquad (5)$$

In [41], the proportional K_{pc} and integral K_{ic} gains of inner current control $G_c(s)$ are achieved through pole placement to achieve pole-zero cancellation. The tuning method employed in this paper relies on an optimization algorithm.

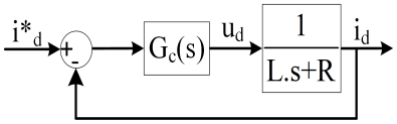

Figure 5. The current control loop diagram.

3.2. Outer Voltage Control

The closed-loop transfer function for the current control loop is:

$$H_{bf}(s) = \frac{\frac{k_{pc}}{k_{ic}}s + 1}{\frac{L}{k_{ic}}s^2 + \frac{R}{k_{ic}}s + (\frac{k_{pc}}{k_{ic}}s + 1)} \qquad (6)$$

To facilitate the voltage controller tuning, the closed-loop transfer function for the current control loop can be approximated by a simplified first-order pole with reduced order.

Since in higher frequencies, $\frac{k_{pc}}{k_{ic}}s >> 1$

then $\frac{k_{pc}}{k_{ic}}s + 1 = \frac{k_{pc}}{k_{ic}}$.

Therefore, $H_{bf}(s) = \frac{k_{pc}}{Ls + R + k_{pc}} = \frac{k}{1 + \tau s}$ (7)

Where $k = \frac{k_{pc}}{R + k_{pc}}$ and $\tau = \frac{L}{R + k_{pc}}$

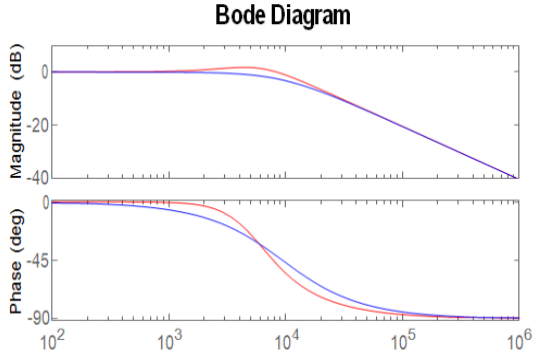

Figure 6. Comparison between frequency responses of approximated and original closed-loop voltage control transfer function.

Figure 6 illustrates the comparison of Bode plots, highlighting the similarity between the approximated and original transfer functions in terms of frequency response at the voltage outer loop bandwidth of ω_v = 1000 rad/s.

Figure 7 showcases the closed voltage control loop where a FO-PI controller is proposed to regulate the output voltage.

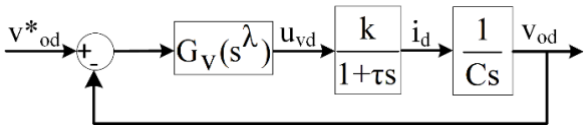

Figure 7. Schematic of the Voltage control loop.

The PI voltage controller is defined as:

$$G_v(s) = K_{pv} + \frac{K_{iv}}{s} \qquad (8)$$

However, the FO-PI voltage controller is defined as:

$$G_v(s) = K_{pv}(1 + \frac{K_{iv}}{s^{\lambda}}) \qquad (9)$$

where λ is the integrator order

3.3. Optimization Problem

MGs often face uncertainties in load and supply parameters, which is why it is crucial to ensure reliable and stable operation even in the presence of these uncertainties. The stability of MGs is directly influenced by the controller's parameters. Therefore, to fix this issue, an optimization problem is formulated using a transfer function model and solved using an optimization technique.

Various optimization techniques have been developed to tackle nonlinear problems and address these challenges. However, these techniques have certain limitations. They are generally classified based on the search space and objective function, such as Linear Programming (LP), Nonlinear Programming (NLP), and Dynamic Programming (DP). Computational intelligence-based techniques, such as Genetic Algorithm (GA) and Particle Swarm Optimization (PSO), have been proposed to tackle optimization problems [40]. Constrained optimization methods have also been employed in controller design in numerous studies [41] [42] [43]. Including constraints in the control system design can improve its performance and ensure its robustness against uncertainties and load variations.

In this study, the Fmincon function in MATLAB is used to handle input Hessians in different ways, including interior point, active set, and sequential quadratic programming. The selection of the interior-point algorithm is motivated by its

capability to efficiently solve large-scale optimization problems and its well-known faster convergence compared to other algorithms [44]. Figure 8 represents the flowchart of the interior-point algorithm used by the Fmincon solver.

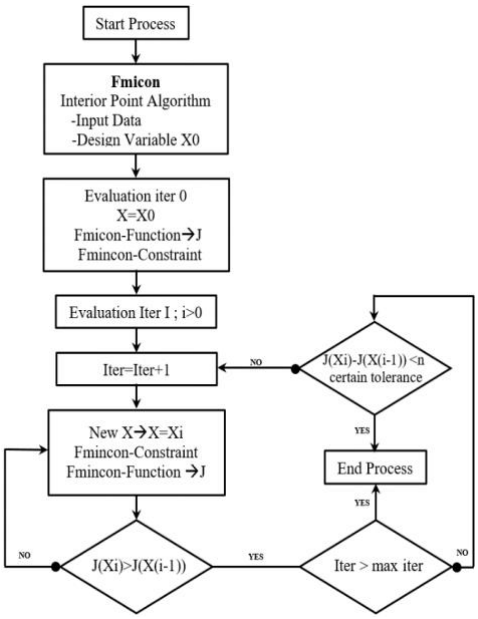

Figure 8. Interior-point algorithm flowchart.

The problem is defined as follows: "Minimize equation (10) subject to the constraints described by equations (11) and (12)", where X_0 represents the initial variable vector, and X represents the optimal variable vector.

The key specifications for tuning the controller's parameters are associated with the phase margin (φm) and the unity-gain frequency(ωu).

To guarantee robustness against variations in system gain, a constraint is imposed to ensure that the open-loop system has a steady phase around the unity-gain frequency (ωu). This constraint enhances the system's resilience to gain fluctuations, and it is mathematically expressed as:

$$\left|H(j\omega_u)C(j\omega_u)\right|_{dB} = 0 \quad (10)$$

$$arg(H(j\omega_u)C(j\omega_u)) = -180 + \varphi_m \quad (11)$$

$$\left.\frac{d(arg(H(j\omega_u)C(j\omega_u)))}{d\omega}\right|_{\omega=\omega_u} = 0 \quad (12)$$

The IO-PI and FO-PI analytical controller parameters for the current and voltage controllers are presented in Table 2.

4. Simulation Results

In this section, a detailed analysis of the newly developed FO-PI control strategy is elaborated to evaluate its performance and robustness. Simulations were carried out using the MATLAB/Simulink Sim Power Systems environment considering an abrupt change in the resistive load and several uncertainties such as voltage reference variations, deviations of filter parameters, and disturbances of the non-linear loads. A comparative study with a conventional PI controller was also carried out. The controller's parameters obtained by applying the proposed optimization method, presented in the previous section, as well as the system parameters and the desired performance are presented in Table 3.

Table 3. System specifications.

Parameters	Notation	Value	Unit
System			
DC input voltage	Vdc	700	V
Frequency	f_s	50	Hz
Nominal voltage	V	380	V
Filter Inductance	L	3.125	mH
Filter resistance	R	0.1	Ω
Filter Capacitor	C	50	μF
Switching frequency	f_s	4	kHz
Desired performance			
Desired ξ	ξ	0.707	-
Desired phase margin	$\phi_m(^\circ)$	70	rad
Unity gain frequency	ω_v	1000	$rad.s^{-1}$
Current Controller			
Proportional	Kpc	29.3312	-
Integral	Kic	$1.0782e^5$	s^{-1}
Voltage Integer Controller			
Proportional	Kpv	0.85	-
Integral	Kiv	12.1535	s^{-1}
Voltage Fractional Controller			
Proportional	Kpv	0.0389	-
Integral	Kiv	19.73	s^{-1}
Lambda	Λ	0.5635	-

Table 2. Controller parameter tuning

	IO-PI controller	FO-PI controller
Transfer function	$C(s) = K_p + \frac{K_i}{s}$	$C(s) = K_p(1 + \frac{K_i}{s^\lambda})$
Constraint (10)	$\left|H(j\omega_u)C(j\omega_u)\right| = K\frac{\sqrt{K_p^2 + (\frac{Ki}{\omega_u})^2}}{\sqrt{1+\tau^2\omega_u^2}} = 1$	$KK_p\frac{\sqrt{(1+K_i\omega_u^{-\lambda}cos(\frac{\lambda\pi}{2}))^2 + (K_i\omega_u^{-\lambda}sin(\frac{\lambda\pi}{2}))^2}}{\sqrt{1+\tau^2\omega_u^2}} = 1$

Constraint (11)	$tan^{-1}(\frac{k_i}{\omega_u k_p}) - tan^{-1}(\tau\omega_u) - T\omega_u = -180 + \varphi_m$	$\frac{K_i\omega_u^{-\lambda}sin(\frac{\lambda\pi}{2})}{1+K_i\omega_u^{-\lambda}cos(\frac{\lambda\pi}{2})} = tan(tan^{-1}(\lambda\omega_u + T\omega_u + \varphi_m))$

Based on the specific controller parameters listed in Table 3, the voltage open-loop Bode diagrams system controlled with the IO-PI and FO-PI controller are presented in Figure 9.

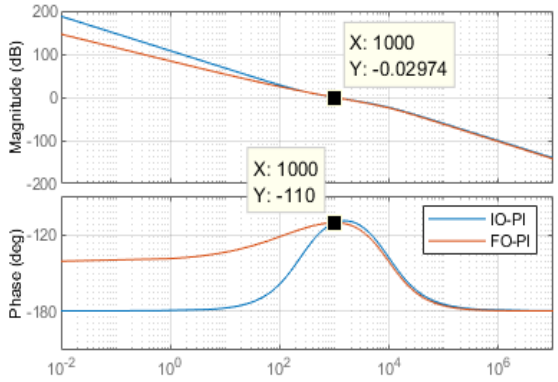

Figure 9. Open-loop system's Bode diagrams.

It is shown that at the desired frequency ω_v=1000rad/s, the phase margin is identical to the desired one, and the gain at ω_u frequency approaches zero.

The fractional order PI controller satisfies the constraint (12) and maintains a nearly constant value while exhibiting a relatively flat phase profile around the ω_u.

The controlled system enhanced the robustness with the optimal choice of the parameter λ, surpassing the performance of the IO-PI controller in providing a wide range of stability.

The reliability of the proposed control technique is improved by including varied disturbances and uncertainties.

4.1 *High Resistive Load Variation*

Initially, a 5 kW resistive load is connected to the voltage source inverter, then, an abrupt voltage disturbance is created at t = 0.15s, by switching "ON" a 10 kW resistive load.

Sudden alterations in the connected load can cause significant instability and perturbation within the controlled system. This negatively affects the system's performance and leads to various problems such as harmonics, poor power factor, and fluctuations in load voltage magnitudes.

Figure 10 illustrates the output power curve, which demonstrates that the FO-PI controller successfully generates the desired load power demand.

Unlike the IO-PI controller, the observed behavior with the FO-PI shows a smooth transition from 5 kW to 10 kW and exhibits less overshoot.

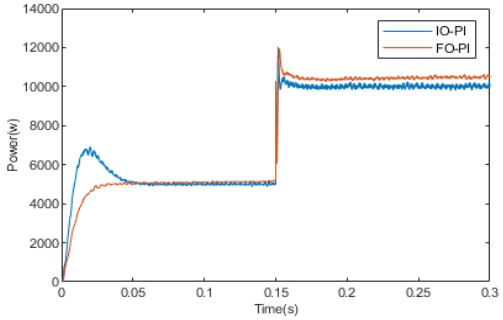

Figure 10. Power output is given by the fractional controller (red) and the conventional controller (blue) in case of a high resistive load variation.

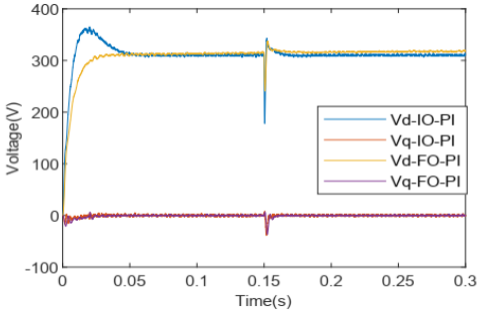

Figure 11. d-axe voltage output given by the fractional and conventional controllers in case of a high resistive load variation.

Figure 11 depicts voltage output in the d-q axis applying integer and fractional PI controllers. The FO-PI controller succeeds in reducing overshoot, particularly in voltage and power transients. It also exhibits greater current and voltage output quality than the PI controller, as represented in Figure 12 and Figure 13, respectively.

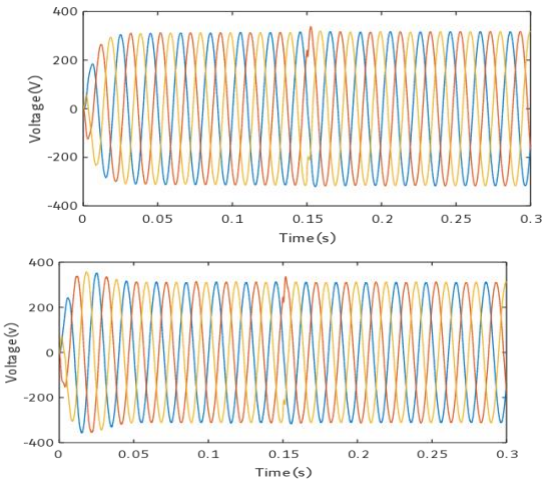

Figure 12. (a) Load voltage with FO-PI controller and (b) Load voltage with IO-PI controller in case of a high resistive load variation.

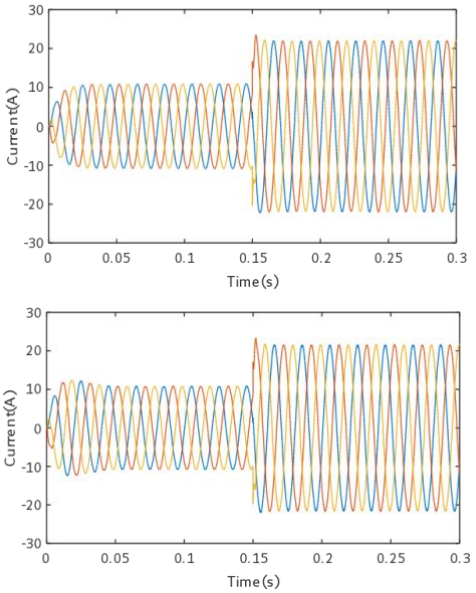

Figure 13. (a) Load current with FO-PI controller and (b) Load current with IO-PI controller in case of a high resistive load variation.

4.2 Voltage Reference Tracking

To assess the tracking effectiveness of the suggested fractional controller, a disturbance was added to the voltage reference input. The nominal voltage value was reduced by 10% from 310 V to 280 V.

Figure 14 displays the voltage output tracking in response to this perturbation for both treated controllers. The Fractional order controller demonstrates a rapid response time, reduced undershoot during the transitional phase and reduced settling time compared to the PI controller.

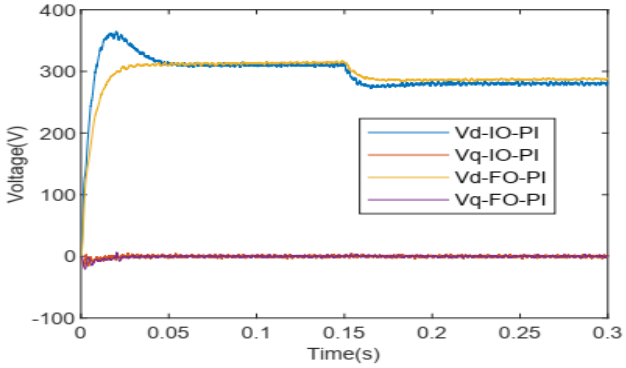

Figure 14. Voltage output tracking with IO-PI and FO-PI in case of a voltage input disturbance.

Figure 15 and Figure 16 exhibit the load current and voltage output, respectively, using the suggested controllers. The perturbation in the voltage reference amplifies the total harmonic distortion in both the current and voltage output. The proposed FO-PI exhibits lower harmonic distortion than the IO-PI controller, particularly during the perturbation phase.

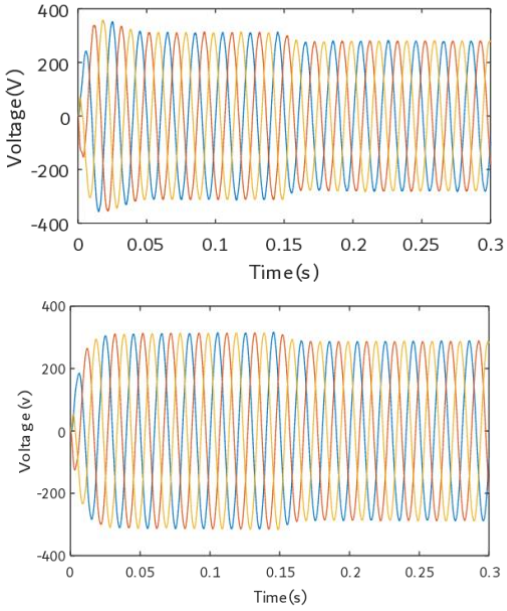

Figure 15. (b) Load voltage with FO-PI controller and (b) Load voltage with IO-PI controller in case of a voltage input disturbance.

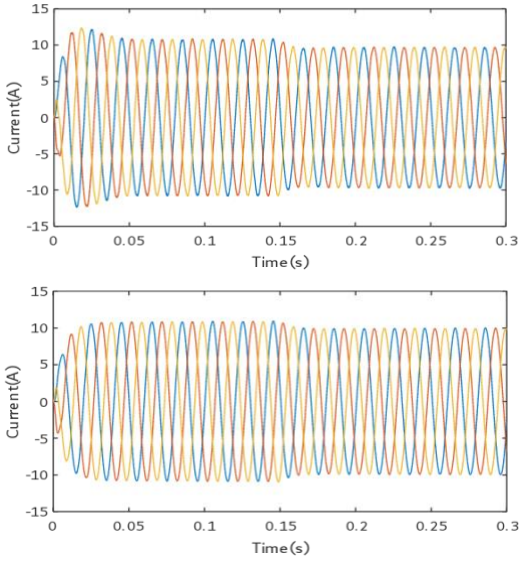

Figure 16. (a) Load current with FO-PI controller and (b) Load current with IO-PI controller in case of a voltage input disturbance.

4.3 Filter Parameters Variations

Harmonic filter circuits are specifically designed to mitigate the presence of harmonic currents in the power system. Their main objective is to reduce the flow of harmonics originating from the power source, thereby alleviating the distortion caused by harmonic voltages within the system.

The variation of the filter parameters can significantly affect the system damping, particularly when the phase margin is reduced. Intending to evaluate the robustness of the suggested fractional PI, the inductance (L) and resistance (R) parameters of the VSC filter are modified. Figure 17 and

Figure 18 illustrate the THD of the voltage output using IO-PI and FO-PI controllers for two different sets of filter parameters. The parameter values of L and R are adjusted from $L = 3.125$ e-3H and $R = 0.1$ Ω to $L = 6.5$ e-3H and $R = 0.2$ Ω.

- For L = 3.125e-3H and R = 0.1Ω

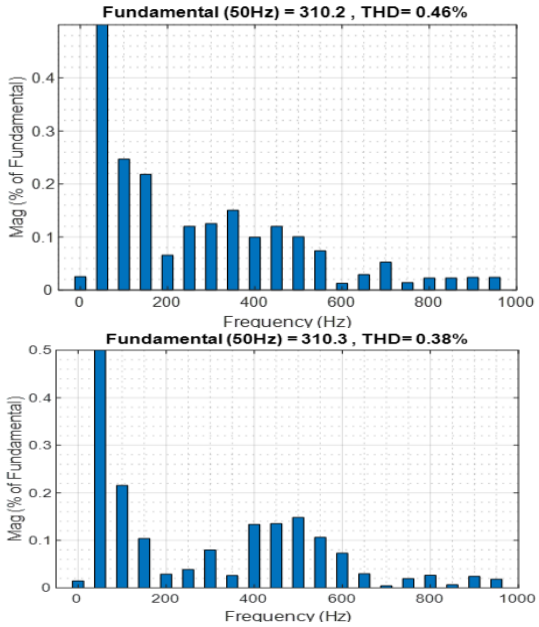

Figure 17. (a) Voltage output THD with IO-PI controller (b) Voltage output THD with FO-PI controller.

- For L = 6.5 e-3H and R = 0.2Ω

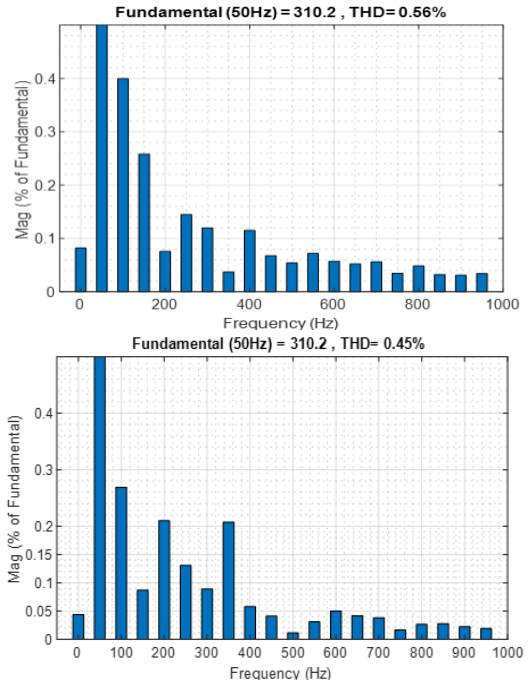

Figure 18. (a) Voltage output THD with IO-PI controller (b) Voltage output THD with FO-PI controller.

The THD values for the voltage output with the FO-PI controller are measured at 0.38% and 0.45%, while with the IO-PI controller, they are recorded as 0.46% and 0.56%.

The proposed fractional PI controller demonstrates reduced THD in both current and voltage than the PI controller.

Despite that the filter parameters variation leads to modifications in the system damping, the FO-PI controller enhances robustness against system uncertainties and filter parameters variations.

4.4 Nonlinear Load Variation

The voltage source controller is connected to a linear load and leads to the production of sinusoidal currents and voltages at a single frequency. The power factor is solely determined by the phase disparity between the current and voltage.

However, the introduction of nonlinear load types causes a deviation in the current waveform from a pure sine wave, resulting in the manifestation of different types of waveforms. Figure 19 presents a schematic of a nonlinear load.

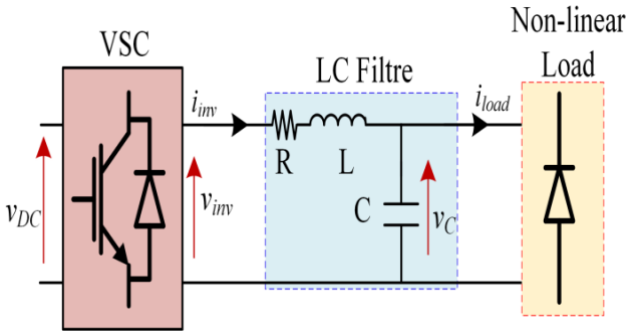

Figure 19. Schematic of the nonlinear load.

The presence of non-linear loads introduces harmonic currents in the fundamental frequency AC.

The THD of the voltage waveform, considering PI and FO-PI controllers, is observed in Figure 20. Figure 21 illustrates the behavior of the system upon connection to a non-linear load.

Non-linear loads cause a deviation in the current and voltage waveform from a pure sine wave, as depicted in Figure 21, by introducing additional harmonics.

The IO-PI controller exhibits an increase in voltage harmonic distortion from 0.46% to 2.01%, while the THD with the FO-PI controller increases from 0.38% to 1.75%, compared to the linear load condition.

The FO-PI controller demonstrates enhanced robustness against harmonic distortion, particularly when the system is connected to a non-linear load when compared to the conventional PI controller.

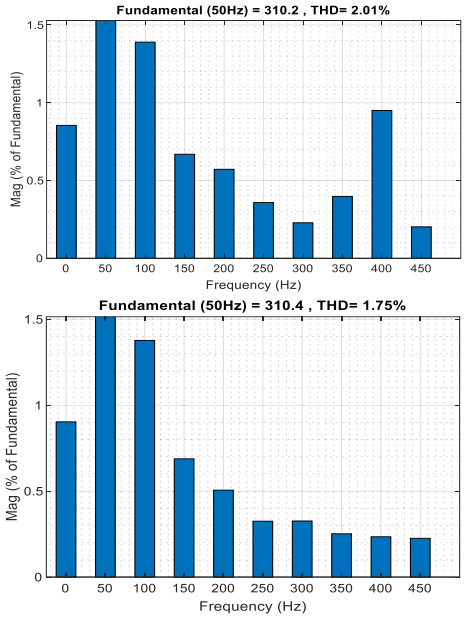

Figure 20. (a)Voltage output THD with IO-PI controller and (b)Voltage output THD with FO-PI in case of a nonlinear load.

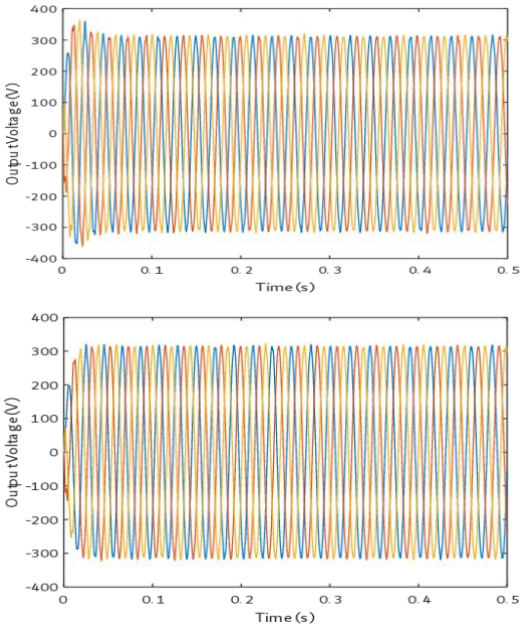

Figure 21. (a)Voltage output with IO-PI controller and (b)Voltage output with FO-PI in case of a nonlinear load.

5. Conclusion

In this study, a robust control strategy was developed for three-phase standalone MGs with a single power source. It consists of a Fractional Order-PI (FO-PI) controller which integrates the inner current and voltage control and whose parameters are adjusted through a constrained optimization approach. The global system was implemented and simulated using MATLAB/Simulink software. To evaluate the proposed controller's effectiveness, various simulation tests are conducted, including disturbances caused by high resistive loads, changes in voltage references, variations in filter parameters, and switching of nonlinear loads. The performance of the proposed controller was compared with that of a conventional PI controller. The fractional controller exhibits superior performance in terms of robustness against load variations and uncertainties in system parameters. Moreover, it achieves a reduction in total harmonic distortion of 0.45% in the case of a system connected to a linear load and 1.75% in the presence of a nonlinear load.

Based on this work, there are several potential research avenues to explore. Firstly, it is recommended to conduct a comparative study between the proposed robust control approach and other robust control methods, such as CRONE and H-infinity control. This comparison would provide further information on the performance and effectiveness of the proposed approach.

Additionally, experimental validation of the proposed controller can be carried out to assess its performance in real-world scenarios. As a practical application, the proposed controller can be used for smart microgrids with multiple sources. Besides its application in microgrid control, the proposed controller can be applied to other different fields such as speed control of an induction motor and electric vehicle (EV) traction. The major disadvantage of FOPI controllers is that are more difficult to implement, and tune compared to classical PI controllers.

Furthermore, it is possible to extend the application of the FO-PI controller to the management of complex MGs involving multiple objectives and constraints. This could open new avenues for research and contribute to the advancement of microgrid control techniques.

References

[1] K. A. Tahir, M. Zamorano and J. O. García “Scientific mapping of optimisation applied to microgrids integrated with renewable energy systems”, International Journal of Electrical Power & Energy Systems, vol. 145, pp. 108698, 2023.

[2] H. Adam, P. Yael, and G. Josep, “Microgrids: A review of technologies, key drivers, and outstanding issues”, Renewable and Sustainable Energy Reviews, vol.90, pp. 402–411, 2018.

[3] I. Worighi, A. Maach, A. Hafid, O. Hegazy, and J. Van Mierlo, “Integrating renewable energy in smart grid system: Architecture, virtualization and analysis”, Sustainable Energy, Grids and Networks, vol. 18, pp. 100226, 2019.

[4] W. F. Mbasso, R. J. J. Molu, S. R. D. Naoussi and S. K. TSOBZE, S. K. “A Technical Analysis of a Grid-Connected Hybrid Renewable Energy System under Meteorological Constraints for a Timely Energy Management”, International Journal of Smart Grid, Vol. 7(2), pp. 53-60, 2023.

[5] P. Mathiesen, M. Stadler, J. Kleissl and Z. Pecenak, “Techno-economic optimization of islanded microgrids

considering intra-hour variability". Applied Energy, vol. 304, pp. 117777,2021.

[6] I. Khan, A.S. Vijay and S. Doolla, "Nonlinear Load Harmonic Mitigation Strategies in Microgrids: State of the Art". IEEE Systems Journal, vol. 16, pp. 4243–4255, 2022.

[7] S. Chreang and P. Kumhom, "A study of nonlinear DC and AC loads connected to PV microgrid", 2018 5th International Conference on Business and Industrial Research, IEEE, pp.309–313,2018.

[8] S. Ullah, A.Haidar, P. Hoole, S.Ullah, A. M. Haidar, P. Hoole, H. Zen and T. Ahfock "The current state of Distributed Renewable Generation, challenges of interconnection and opportunities for energy conversion based DC microgrids", Journal of Cleaner Production, vol. 273, pp. 122777, 2020.

[9] IEEE Std 1159-2009, "IEEE Recommended Practice for Monitoring Electric Power Quality". IEEE Std 1159-2009 (Revision of IEEE Std 1159-1995), pp. 1–94, 2009.

[10] IEEE Std 141-1993, "IEEE Recommended Practice for Electric Power Distribution for Industrial Plants". IEEE Std 141-1993, pp. 1–768, 1994.

[11] B. Modu, , M. P. Abdullah, M. A.Sanusi, and Hamza, M. F. "DC-Based microgrid: Topologies, control schemes, and implementations", Alexandria Engineering Journal, Vol 70, pp.61-92, 2023.

[12] F. Mansouri Kouhestani, J. Byrne, D. Johnson, L. Spencer,B. Brown, P. Hazendonk, and J. Scott, J. "Multi-criteria PSO-based optimal design of grid-connected hybrid renewable energy systems", International Journal of Green Energy, vol 17(11), pp.617-631, 2020.

[13] Y. Tzou, S.L. Jung and H. Yeh, "Adaptive repetitive control of PWM inverters for very low THD AC-voltage regulation with unknown loads". IEEE Transactions on Power Electronics, vol. 14, pp. 973–981, 1999.

[14] D.U. Kalla, B. Singh, S. Murthy, C. Jain, and K. Kant, "Adaptive Sliding Mode Control of Standalone Single-Phase Microgrid Using Hydro, Wind and Solar PV Array Based Generation", IEEE Transactions on Smart Grid, vol.9, pp. 6860–6814, 2016.

[15] M. A. E. Alali, Z. Sabiri, Y. B. Shtessel and J. P. Barbot, "Study of a common control strategy for grid-connected shunt active photovoltaic filter without DC/DC converter", Sustainable Energy Technologies and Assessments, Vol 45, pp 101149, 2021.

[16] J. Arkhangelski, M. Abdou-Tankari and G. Lefebvre "Efficient abnormal building consumption detection by deep learning LSTM IOT data classification", 11th International Conference on Renewable Energy Research and Application (ICRERA), pp. 125-129, IEEE, September 2022.

[17] MM. Gulzar, "Designing of robust frequency stabilization using optimized MPC-(1+ PIDN) controller for high order interconnected renewable energy-based power systems", Protection and Control of Modern Power Systems, vol. 8, pp. 1-14, 2023.

[18] K., N., Houari, A., Ait-Ahmed, M. Machmoum, and M. Ghanes, "Robust IDA-PBC Based Load Voltage Controller for Power Quality Enhancement of Standalone Microgrids". IECON 2018 - 44th Annual Conference of the IEEE Industrial Electronics Society, pp. 249–254, 2018.

[19] D. Datta, S. K. Sarker and M. R. I. Sheikh, "Designing a unified damping and cross-coupling rejection controller for LCL filtered PV-based islanded microgrids", Engineering Science and Technology, an International Journal, 35, 101244, 2022.

[20] M. Hamzeh, S. Emamian, H. Karimi, and J. Mahseredjian, "Robust Control of an Islanded Microgrid Under Unbalanced and Nonlinear Load Conditions", IEEE Journal of Emerging and Selected Topics in Power Electronics, vol.4, pp. 512–520, 2016.

[21] A. Sinha, and K.C. Jana, "Comprehensive review on control strategies of parallel-interfaced voltage source inverters for distributed power generation system" IET Renewable Power Generation, vol. 14, pp. 2297–2314, 2020.

[22] D. Chen, J. Zhang, and Z. Qian, "An Improved Repetitive Control Scheme for Grid-Connected Inverter with Frequency-Adaptive Capability", IEEE Transactions on Industrial Electronics, vol. 60, pp. 814–823, 2013.

[23] S. R. Basavarajappa and M. S. Nagaraj, "Load frequency control of three area interconnected power system using conventional PID, fuzzy logic and ANFIS controllers", 2nd International Conference for Emerging Technology (INCET). IEEE, pp. 1-6, 2021.

[24] A. Dkhil, M. Chetoui, and M. Amairi, "Optimization-based tuning of a Robust PI current controller for a three-phase grid connected PV system". 2019 International Conference on Signal, Control, and Communication (SCC), pp. 150–155, 2019.

[25] A. Dkhil, M. Chetoui, and M. Amairi, "Optimization-based design of fractional PI controller for a three-phase grid connected PV system", 2020 17th International Multi-Conference on Systems, Signals, and Devices (SSD), pp. 440–445, 2020.

[26] T., A. M., Hasanien, H. M., Ginidi, A. R., and A. T. Taha "Hierarchical model predictive control for performance enhancement of autonomous microgrids", Ain Shams Engineering Journal, Vol. 12(2), pp. 1867-1881, 2021.

[27] B. Zhang and Y. Pi, "Enhanced robust fractional order proportional-plus-integral controller based on neural

network for velocity control of permanent magnet synchronous motor", ISA transactions, vol. 52, pp.510–516, 2013.

[28] V. Suresh, N. Pachauri, and V. Thangavel, "Decentralized control strategy for fuel cell/PV/BESS based microgrid using modified fractional order PI controller", International Journal of Hydrogen Energy, vol.46, pp.4417–4436, 2021.

[29] V. Rajaguru and K. I. Annapoorani, "Virtual synchronous generator based superconducting magnetic energy storage unit for load frequency control of micro-grid using African vulture optimization algorithm", Journal of Energy Storage, vol. 65, pp. 107343, 2023.

[30] M. Ortiz-Quisbert, M. Duarte-Mermoud, F. Milla, R. Castro-Linares and G. Lefranc, "Optimal fractional-order adaptive controllers for AVR applications", Electrical Engineering, vol.100, pp.267–283, 2018.

[31] R. Abdulkader and R. McCann, "Fractional Order PI Control for a Three-Phase Microgrid Application", 2018 Clemson University Power Systems Conference (PSC), pp. 1–4, 2018.

[32] M. Zolfaghari, A. K. Arani, G. B. Gharehpetian, and M. Abedi, "Fractional order proportional-integral controller design to improve load sharing between DGs in microgrid", 2016 Smart Grids Conference (SGC), pp. 1–5, 2016.

[33] D. Pullaguram, S. Mishra, N. Senroy and M. Mukherjee, "Design and Tuning of Robust Fractional Order Controller for Autonomous Microgrid VSC System", IEEE Transactions on Industry Applications, vol. 54, pp. 91–101, 2018.

[34] F. Bekraoui, I. Colak, A. Bekraoui, K. Roummani, K. and A. Harrouz, "Comparative Study Between the Sliding Mode and Backstepping Current Control of a Grid-Connected Direct Drive Wind-Pmsg System", In 2023 11th International Conference on Smart Grid (icSmartGrid) (pp. 1-10). IEEE, June 2023.

[35] A. Tabak "Fractional order frequency proportional-integral-derivative control of microgrid consisting of renewable energy sources based on multi-objective grasshopper optimization algorithm", Transactions of the Institute of Measurement and Control, Vol 44(2), pp. 378-392, 2022.

[36] B. Singh and S. K. Bishnoi, "Bull-lion Optimization-based Proportional Integrated Derivative controller for regulating frequency in Two-Area Multi-Source power system", Advances in Engineering Software, Vol. 181, pp. 103444, 2023.

[37] A. A. Mahmoud, A. A. Hafez, A. M. Yousef, M. A. Gaafar, M. Orabi and A. F. Ali, "Fault-tolerant modular multilevel converter for a seamless transition between stand-alone and grid-connected microgrid", IET Power Electronics, Vol. 16(1), pp. 11-25, 2023.

[38] I. Carugati, C.M. Orallo, S. Maestri, P.G. Donato, and D. Carrica, "Variable, fixed, and hybrid sampling period approach for grid synchronization", Electric Power Systems. Research, vol. 144, pp. 23-31, 2017.

[39] A. Oymak and M. R. Tur, "A Short Review on the Optimization Methods Using for Distributed Generation Planning", International Journal of smart grid, 6(3), 54-64, 2022.

[40] C. Zhao, X. Lu, and G. Li, "Parameters Optimization of VSC-HVDC Control System Based on Simplex Algorithm", 2007 IEEE Power Engineering Society General Meeting, pp. 1–7, 2007.

[41] D. Saha, N. Bazmohammadi, J. M. Raya-Armenta, A. D. Bintoudi, A. Lashab, J. C. Vasquez, and J. M. Guerrero "Optimal Sizing and Siting of PV and Battery Based Space Microgrids Near the Moon's Shackleton Crater", IEEE Access, vol. 11, pp. 8701-8717, 2023.

[42] R.Yang, Y. Liu, Y. Yu, X. He and H. Li, "Hybrid improved particle swarm optimization-cuckoo search optimized fuzzy PID controller for micro gas turbine", Energy Reports, 7, 5446-5454, 2021.

[43] A. Messac, Optimization in Practice with MATLAB®: For Engineering Students and Professionals, Cambridge University Press, 2015.

[44] D. Tungadio, R. Bansal and M. Siti, "Optimal Control of Active Power of Two Micro-Grids Interconnected with Two AC TiLines", Electric Power Components and Systems, vol. 45, pp. 1-12, 2018.

[45] L. Alhmoud and M. Shloul "Impact of wheeling photovoltaic system on distribution low voltage feeder", Results in Engineering, pp.101378, 2023.

[46] J. Hmad, A. Houari, A. Bouzid, A. Saiem and H. Trabelsi, "A review on mode transition strategies between grid-connected and standalone operation of voltage source inverters-based microgrids", Energies, vol. 16, no 13, pp. 5062, 2023.

[47] J. Hmad, A. Houari, H. Trabelsi, and M. Machmoum, "Fuzzy logic approach for smooth transition between grid-connected and stand-alone modes of three-phase DG-inverter", Electric power systems research, vol. 175, p. 105892, 2019.